Available online at www.sciencedirect.com

SciVerse ScienceDirect

Ceramics International 38 (2012) 1605–1610

CERAMICS INTERNATIONAL

www.elsevier.com/locate/ceramint

Efficient photocatalytic activity of MnO_2-loaded ZrO_2/carbon cluster nanocomposite materials under visible light irradiation

H. Matsui [a], N. Bandou [a], S. Karuppuchamy [b,*], M.A. Hassan [b], M. Yoshihara [a]

[a] Department of Applied Chemistry, Faculty of Science and Engineering, Kinki University, 3-4-1, Kowakae, Higashiosaka, Osaka 577-8502, Japan
[b] Institute of Bioscience, Universiti Putra Malaysia, 43400 Serdang, Selangor, Malaysia

Received 15 September 2011; received in revised form 26 September 2011; accepted 26 September 2011
Available online 1 October 2011

Abstract

Nano-sized ZrO_2/carbon cluster nanocomposite material was successfully prepared by the calcination of $Zr(acac)_4$/epoxy resin complex in air. The composite material obtained by calcining at 200 °C was treated with hydrogen hexachloroplatinate hexahydrate (H_2PtCl_6) to obtain Pt-loaded materials denoted as Ic_{200}Pt'sH's. The Pt-loaded material modified with MnO_2 particles efficiently decompose water into H_2 and O_2 with a $[H_2]/[O_2]$ ratio of 2 under the irradiation of visible light ($\lambda > 460$ nm) through the electron transfer process of $MnO_2 \rightarrow$ carbon clusters $\rightarrow ZrO_2 \rightarrow$ Pt.

Keywords: Carbon; Polymer; Nanostructure; Characterization

1. Introduction

Construction of a charge-separated electron excitation under visible-light irradiation is important to achieve new types of photo-sensitive catalysts for H_2 production from water, CO_2 fixation, solar cell production, and so on. However, an electron transport under whole visible light irradiation has not been established yet [1–6]. We assumed that the composites containing nano-sized semiconductors and carbon clusters may be sensitive to visible light. We recently synthesized and reported such nanocomposite materials by the calcination of both metal-organic moiety hybrid copolymers and inorganic metal compound/organic polymer complexes [7–19]. The visible light-responsive electron transfer between carbon phases and metal compounds was observed for those reported novel composite materials. Especially, CeO_2/carbon clusters/Ho_2O_3 composite material loaded with Pt particles showed the decomposition of water to O_2 and H_2 with a $[O_2]$:$[H_2]$ ratio of 1:2 under visible light irradiation through a two-step electron transfer in the process of $CeO_2 \rightarrow$ carbon clusters $\rightarrow Ho_2O_3 \rightarrow$ Pt [15]. This observation clearly indicates that smooth electron transfer could be achieved by the combination of two metal oxides with different electron moving features, i.e., $(\text{metal oxide})_A \rightarrow$ carbon clusters and carbon clusters $\rightarrow (\text{metal oxide})_B$. We expect that such an electron transfer may also be achieved on the surface of the composite materials with an electron moving feature of carbon clusters $\rightarrow (\text{metal oxide})_B$. We recently reported that the electron transfer process in ZrO_2/carbon clusters composite material is in the direction of carbon clusters $\rightarrow ZrO_2$ [17]. Moreover, MnO_2 is known to be a typical metal oxide with high oxidation ability [20]. Therefore, the combination of MnO_2 particles and ZrO_2/carbon clusters composite material is expected to give rise to a smooth electron transfer feature, possibly through the electron transfer process of $MnO_2 \rightarrow$ carbon clusters $\rightarrow ZrO_2$. In the present work, nano-particles of MnO_2 was loaded onto the surface of ZrO_2/carbon clusters composite material Ic which was obtained by the calcination of $Zr(acac)_4$/epoxy resin complex I (Scheme 1), and the electronic behaviors of the composite materials under visible light irradiation were examined.

2. Experimental

2.1. Reagents

Commercially available zirconium acetylacetonate $Zr(acac)_4$, diglycidyl ether of bisphenol A (DGEBA), phthalic

* Corresponding author. Tel.: +60 38946 7593.
E-mail addresses: skchamy@ibs.upm.edu.my, skchamy@gmail.com (S. Karuppuchamy).

0272-8842/$36.00
doi:10.1016/j.ceramint.2011.09.049

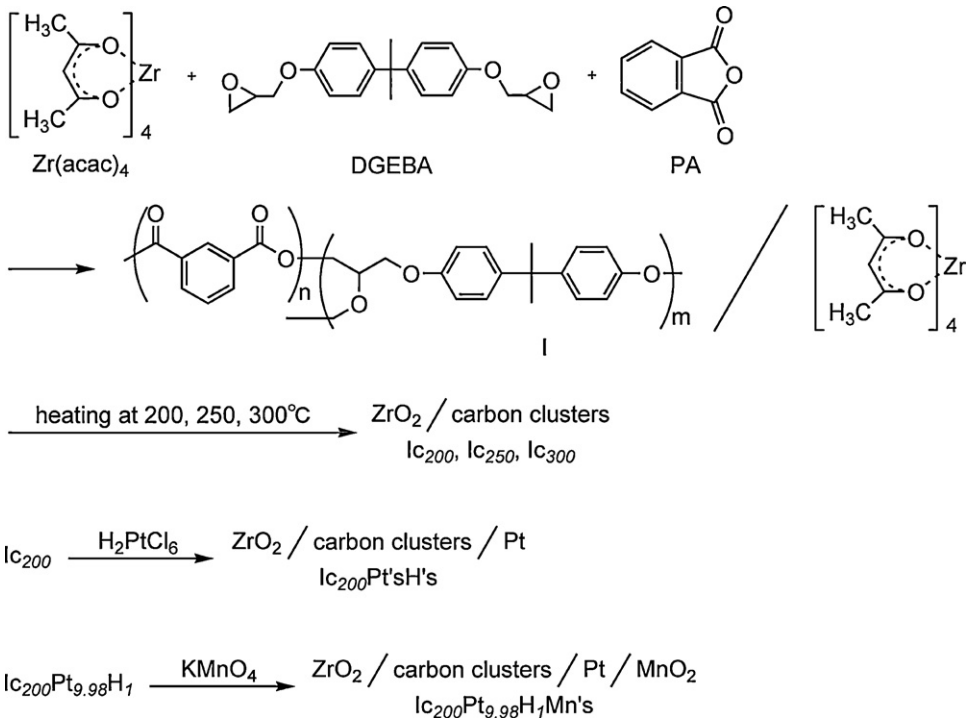

Scheme 1. Synthesis of the materials.

anhydride (PA), $KMnO_4$, methylene blue, citric acid, hydrogen hexachloroplatinate hexahydrate $H_2PtCl_6{\cdot}6H_2O$, 1,4-benzoquinone, and pyrogallol were used as received.

2.2. Synthesis of complex I

10.0 g (20.5 mmol) of $Zr(acac)_4$, 6.96 g (20.5 mmol) of DGEBA and 3.03 g (20.5 mmol) of PA were dissolved in 1.0 L of acetone. Then the acetone was evaporated and subsequently the residues were heated in air at 100 °C for 5 h to obtain complex I.

2.3. Calcination of complex I

1 g of complex I in a porcelain crucible was heated with a heating rate of 5 °C/min under an O_2 atmosphere using a Denken KDF-75 electric furnace and kept at 200, 250 and 300 °C for 3 h to obtain calcined materials denoted as (Ic's) Ic_{200}, Ic_{250} and Ic_{300}, respectively.

2.4. Pt-loading on calcined material Ic_{200}

50 mg of Ic_{200} was added into a mixture of methanol and an aqueous hydrogen hexachloroplatinate hexahydrate solution and then the mixture was deaerated by argon gas bubbling. The charged amounts of reagents are shown in Table 1. The mixture was irradiated by visible light ($\lambda > 460$ nm) for 1, 3 and 6 h. The precipitates were collected, washed with distilled water and dried under a vacuum to obtain a Pt-loaded materials ($Ic_{200}Pt_{1.00–9.98}H_{1–6}$), in which $Pt_{1.00–9.98}$ shows the molar concentration of an aqueous $H_2PtCl_6{\cdot}6H_2O$ solution and $H_{1–6}$ is the light irradiation time.

2.5. MnO_2-loading on $Ic_{200}Pt_{9.98}H_1$

A mixture of 200 mg of $Ic_{200}Pt_{9.98}H_1$, 4 mL of ethanol and varied concentration of [5.75 mg (36.5 μmol), 28.8 mg (182 μmol) and/or 57.5 mg (365 μmol)] $KMnO_4$ was added into 100 mL of water and then the mixture was stirred for 30 min. Then the precipitates were collected, washed with water, dried at 60 °C under a vacuum, and finally the precipitate was heated in a porcelain crucible at 300 °C for 10 min under an air atmosphere to obtain MnO_2-loaded materials $Ic_{200}Pt_{9.98}H_1Mn_{5.75–57.5}$ in which $Mn_{5.75–57.5}$ shows the amount of added $KMnO_4$ in mg.

2.6. Characterization

Elemental analysis was performed for C and H using Yanaco MT-6, and for Zr, Pt and Mn by inductively coupled plasma atomic emission spectrometry (ICP-AES) using Shimadzu ICP-7500. Transmission electron microscopy (TEM) observations were done using a Jeol JEM-3010 microscope. X-ray photoelectron spectra (XPS) were obtained using Shimadzu ESCA-850. Electron spin resonance (ESR) spectra were taken using a Jeol JES-TE200 spectrometer. UV–vis spectra were

Table 1
Charged amounts of an aqueous $H_2PtCl_6{\cdot}6H_2O$ solution and methanol.

Symbols	$H_2PtCl_6{\cdot}6H_2O$	Methanol (mL)
$Ic_{200}Pt_{1.00}H_{1–6}$	2.6 mL of 1.00 mmol/L	2.6
$Ic_{200}Pt_{2.11}H_{1–6}$	1.2 mL of 2.11 mmol/L	1.2
$Ic_{200}Pt_{4.99}H_{1–6}$	0.51 mL of 4.99 mmol/L	0.51
$Ic_{200}Pt_{9.98}H_{1–6}$	0.26 mL of 9.98 mmol/L	0.26

measured using a Hitachi U-4000 spectrometer. Visible light was generated using a Hoya-Schott Megalight 100 halogen lamp. The sharp cut filter Y-48 purchased from Hoya Candeo Optronics Co. was used.

The reduction reaction of methylene blue with the obtained materials Ic's and $Ic_{200}Pt_{1.00–9.98}H_{1–6}$ was carried out in the following way. A mixture of 3 mg of the materials and 10 mL of a 0.03 mmol/L methylene blue–0.12 mmol/L citric acid aqueous solution was stirred in the dark for 48 h under an argon atmosphere. The mixture was irradiated with visible light ($\lambda > 460$ nm) and the concentration of methylene blue was determined by UV–vis spectral analysis. The intensity of irradiated visible light was 2 mW/cm^2.

The oxidation–reduction reaction of an aqueous silver nitrate solution with $Ic_{200}Pt_{9.98}H_1$ and $Ic_{200}Pt_{9.98}H_1Mn_{5.75–57.5}$ was also performed in the following way. A mixture of 10 mg of the materials and 1 mL of a 0.05 mmol/L $AgNO_3$ aqueous solution was irradiated by visible light ($\lambda > 460$ nm) under an argon atmosphere for 3 h, and then the evolved O_2 gas was analyzed with Shimadzu GC-8A gas chromatography and the formed Ag was estimated by ICP analysis.

The water splitting experiments were carried out in the following way. A stirred mixture of 0.2 mL of degassed water and 10 mg of $Ic_{200}Pt_{9.98}H_1$ and/or $Ic_{200}Pt_{9.98}H_1Mn_{57.5}$ was irradiated by visible light ($\lambda > 460$ nm) at room temperature for 12 h under an argon atmosphere, and the evolved H_2 and O_2 gases were analyzed by using gas chromatography.

3. Results and discussion

The results of the elemental analysis of complex I and calcined materials Ic's are shown in Table 2, indicating that Zr atom was detected in the materials. The H contents and [C]/[Zr] ratios of Ic's decreased with the increase of calcination temperature, suggesting that the carbonization of the materials successfully proceeded. The XPS measurements of Ic's were found to give a binding energy at 182.2–182.3 eV due to the $3d_{5/2}$ orbital of Zr atom of ZrO_2. The results suggest that the calcined materials were composed of ZrO_2 and carbon clusters.

Table 2
Elemental analysis of complex I and calcined materials Ic's.

Materials	C (%)	H (%)	Zr (%)	[C]:[Zr]
Ic	57.6	5.82	10.3	43:1
Ic_{200}	56.6	4.94	12.3	35:1
Ic_{250}	51.5	3.31	16.5	24:1
Ic_{300}	48.8	2.71	17.7	21:1

The electronic behaviors of the calcined materials were examined. First, the ESR spectra of Ic's were measured and a peak signal at 337 mT ($g = 2.003$) was observed. Our understanding is that an electron transfer between the ZrO_2 particles and the carbon clusters took place to form a free electron on the carbon clusters. Fig. 1 shows the ESR spectra of Ic_{250} in the presence of either an oxidant (1,4-benzoquinone) or a reductant (pyrogallol) under the irradiation of visible light ($\lambda > 460$ nm). The signal intensity was found to increase with the addition of the oxidant but decrease with the addition of the reductant, indicating that the signal is due to a radical cation. It is thus deduced that an electron transfer from the carbon clusters to the ZrO_2 parts takes place. Moreover, the electron transfer between the carbon and oxide occurs in tunneling through the potential barrier at the heterointerface between the carbon cluster and the metal oxide.

The photocatalytic ability of the calcined materials was also examined. Fig. 2 is the UV–vis spectra of methylene blue in the presence of Ic_{200} under the irradiation of visible light ($\lambda > 460$ nm). The absorption band of methylene blue decreases with the increase of the irradiation time, indicating that Ic_{200} has visible light-responsive reduction ability. The reduction activities (*ra*) of Ic_{200}, Ic_{250} and Ic_{300} were determined by the equation *ra* = (the amount of methylene blue) · (g of the calcined material)$^{-1}$ · (h)$^{-1}$ to be 2.20, 0.67 and 0.36 μmol g^{-1} h^{-1}, respectively. The highest *ra* value was

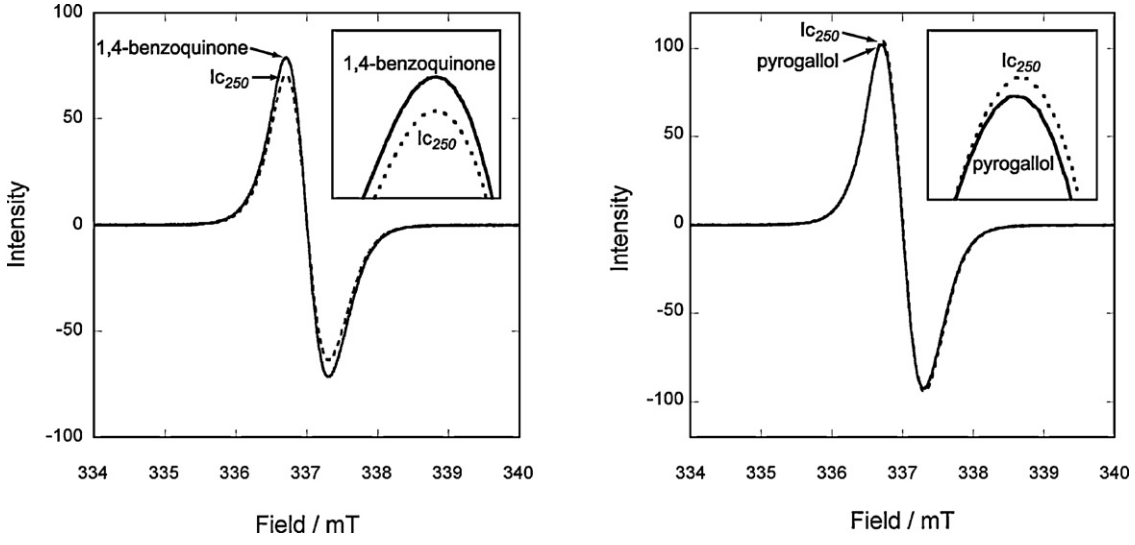

Fig. 1. ESR spectra of Ic_{250} in the presence of 1,4-benzoquinone or pyrogallol.

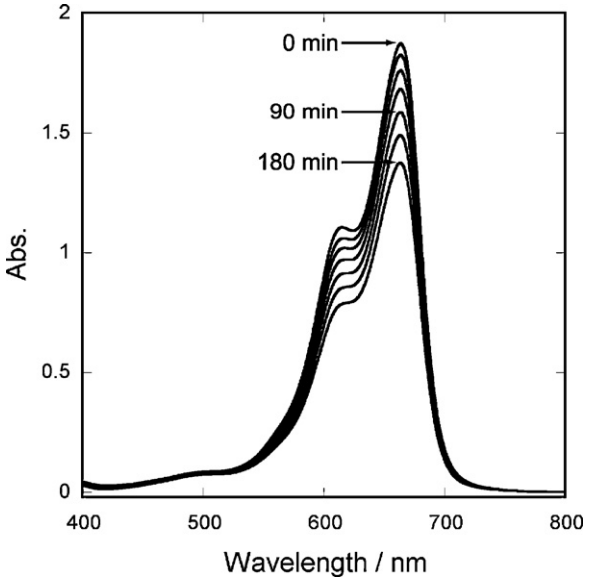

Fig. 2. UV–vis spectra of methylene blue in the presence of Ic_{200} under the irradiation of visible light ($\lambda > 460$ nm).

obtained for Ic_{200}, indicating that Ic_{200} has the highest photo-reduction ability.

It is known that the loading of Pt particles on semiconductors increases the reduction ability. The surfaces of Ic_{200} were thus modified with Pt particles according to the procedures described in Section 2.4 to give Pt-loaded materials $Ic_{200}Pt_{1.00–9.98}H_{1–6}$. The XPS spectra of the obtained materials showed a peak at 70.9–71.1 eV due to the $4f_{7/2}$ orbital of Pt. The Pt contents in the materials were determined by the ICP analysis and the results are summarized in Table 3. The Pt contents were found to increase with the increase of the molar concentrations of hydrogen hexachloroplatinate solution but to be essentially unchanged with the irradiation time. The TEM observations of $Ic_{200}Pt_{1.00–9.98}H_{1–6}$ (Fig. 3) showed that highly densed particles with the diameters of 1–20 nm, possibly Pt particles, were loaded on the surfaces of the materials and the sizes of the particles increased with the increase of either the concentration of hydrogen hexachloroplatinate solution or the

Table 3
Pt contents and reduction activities (*ra*) of Pt-loaded materials $Ic_{200}Pt_{1.00–9.98}H_{1–6}$ and Ic_{200}.

No.	Materials	Pt (%)	*ra* (μmol g^{-1} h^{-1})
1	$Ic_{200}Pt_{1.00}H_1$	0.29	2.91
2	$Ic_{200}Pt_{1.00}H_3$	0.31	3.09
3	$Ic_{200}Pt_{1.00}H_6$	0.32	3.43
4	$Ic_{200}Pt_{2.11}H_1$	0.38	5.43
5	$Ic_{200}Pt_{2.11}H_3$	0.39	5.68
6	$Ic_{200}Pt_{2.11}H_6$	0.41	8.95
7	$Ic_{200}Pt_{4.99}H_1$	0.51	10.3
8	$Ic_{200}Pt_{4.99}H_3$	0.53	4.29
9	$Ic_{200}Pt_{4.99}H_6$	0.53	4.56
10	$Ic_{200}Pt_{9.98}H_1$	0.64	10.9
11	$Ic_{200}Pt_{9.98}H_3$	0.66	8.58
12	$Ic_{200}Pt_{9.98}H_6$	0.67	5.36
13	Ic_{200}	0	2.2

Table 4
Elemental analyses of MnO_2-loaded materials $Ic_{200}Pt_{9.98}H_1Mn_{5.75–57.5}$.

Materials	C (%)	H (%)	Zr (%)	Mn (%)	[C]:[Zr]:[Mn]
$Ic_{200}Pt_{9.98}H_1Mn_{5.75}$	56.6	4.75	14.7	0.56	29:1:0.06
$Ic_{200}Pt_{9.98}H_1Mn_{28.8}$	58.1	4.67	15.5	4.37	28:1:0.47
$Ic_{200}Pt_{9.98}H_1Mn_{57.5}$	56.0	4.62	14.4	9.32	30:1:1.1

irradiation time. The visible light-irradiated reduction reaction of methylene blue with the Pt-loaded materials was examined and the values of reduction activities (*ra*) are also summarized in Table 3. The *ra* values of the Pt-loaded materials (Nos. 1–12) were found to be larger than that of Pt-unloaded material Ic_{200} (No. 13), indicating that the Pt-loading enhanced the reduction ability. It is noted that the highest *ra* value was observed for $Ic_{200}Pt_{9.98}H_1$ (No. 10). At present, we consider that the size of the Pt particles might be an important for the photo-reduction abilities of the materials, since rather larger *ra* values (Nos. 7 and 10 in Table 3) were observed for the materials with the Pt particles size of ca. 5 nm (Nos. 7 and 10 in Fig. 3) while lower *ra* values (Nos. 1–6, 8, 9, 11 and 12 in Table 3) were obtained for the materials with either smaller Pt particles size (Nos. 1, 2 and 4 in Fig. 3) or larger Pt particles size (Nos. 3, 5, 6, 8, 9, 11 and 12 in Fig. 3).

MnO_2 particles with high oxidation ability were loaded on the surface of $Ic_{200}Pt_{9.98}H_1$ according to the procedure described in Section 2.5 to obtain the MnO_2-loaded materials denoted as $Ic_{200}Pt_{9.98}H_1Mn_{5.75–57.5}$. The results of the elemental analysis of the obtained materials are shown in Table 4, indicating that the Mn contents in the materials increased with the increase of the concentration of an aqueous $KMnO_4$ solution. The XPS measurements of the materials showed peaks either at 641.8–642.1 eV due to the $2p_{3/2}$ orbital of Mn atom of MnO_2 or at 182.1–182.4 eV due to the $3d_{5/2}$ orbital of Zr atom of ZrO_2. The TEM observations for the materials showed the presence of particles with the diameters of either ca. 50–100 nm, possibly MnO_2, or ca. 5 nm, possibly Pt, on the surface of the matrix. The visible light-irradiated oxidation-reduction abilities of the MnO_2-loaded materials were examined. First, the visible light-irradiated decomposition reaction of an aqueous silver nitrate solution with MnO_2-loaded materials $Ic_{200}Pt_{9.98}H_1Mn_{5.75–57.5}$ was performed and the results are shown in Table 5. The amounts of O_2 and Ag formed for MnO_2-loaded materials $Ic_{200}Pt_{9.98}H_1Mn_{5.75–57.5}$ (Nos. 1–3) were found to be higher than those for $Ic_{200}Pt_{9.98}H_1$ (No. 4), and the highest O_2 and Ag formation was observed for $Ic_{200}Pt_{9.98}H_1Mn_{57.5}$ (No. 3). Here, if a four electron oxidation-reduction reaction takes place,

Table 5
Amounts of O_2 and Ag in the decomposition reaction of an aqueous silver nitrate solution under the irradiation of light ($\lambda > 460$ nm).

No.	Materials	O_2 (μmol)	Ag (μmol)	Ratio $[O_2]$:[Ag]
1	$Ic_{200}Pt_{9.98}H_1Mn_{5.75}$	56	229	1:4.1
2	$Ic_{200}Pt_{9.98}H_1Mn_{28.8}$	75	313	1:4.2
3	$Ic_{200}Pt_{9.98}H_1Mn_{57.5}$	94	385	1:4.1
4	$Ic_{200}Pt_{9.98}H_1$	46	144	1:3.1

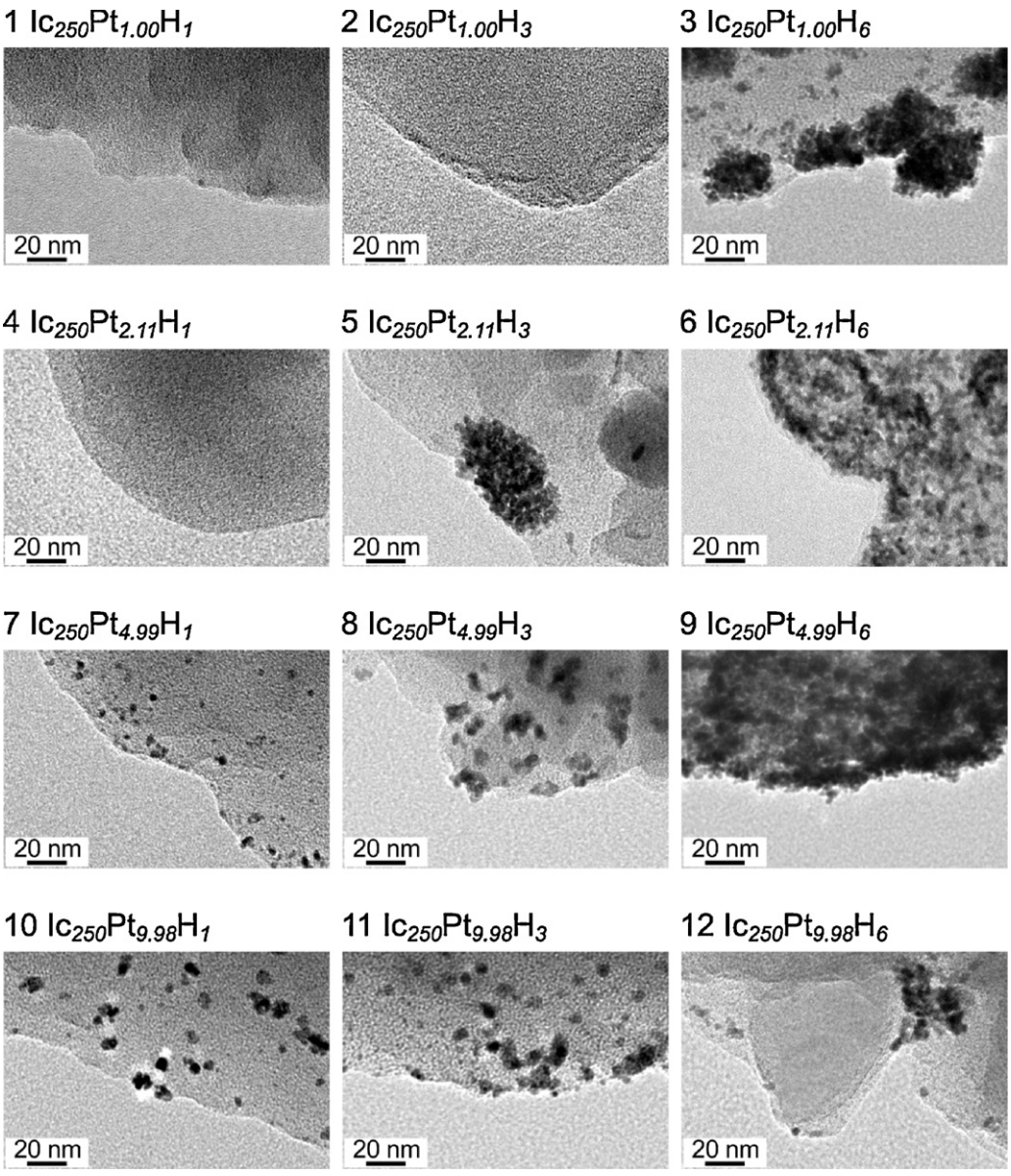

Fig. 3. TEM images of Pt-loaded materials $Ic_{200}Pt_{1.00–9.98}H_{1–6}$.

then a $[O_2]$:[Ag] ratio is given to be 1:4. The $[O_2]$:[Ag] ratios of the MnO_2-loaded materials (Nos. 1–3) were obtained to be nearly 1:4, while the MnO_2-loaded material (No. 4) gave the value of 1:3.1. Next, water splitting experiments with $Ic_{200}Pt_{9.98}H_1$ and $Ic_{200}Pt_{9.98}H_1Mn_{57.5}$ were carried out and the results are shown in Table 6. It is quite interesting to note that O_2 and H_2 were obtained with an $[O_2]$:$[H_2]$ ratio of 1:2 and the amount of H_2 formed for $Ic_{200}Pt_{9.98}H_1Mn_{57.5}$ was higher than that for $Ic_{200}Pt_{9.98}H_1$. Our opinion is that the MnO_2-loading onto the surface of $Ic_{200}Pt_{9.98}H_1$ caused a smooth electron transfer through the electron transfer process of $MnO_2 \rightarrow$ carbon clusters $\rightarrow ZrO_2 \rightarrow$ Pt to enhance the degree of either an oxidation ability at the MnO_2 particles or a reduction ability at the Pt parts, thus facilitating the water decomposition. It is also noted that no evolution of O_2 was observed for $Ic_{200}Pt_{9.98}H_1$. A possible assumption for non-generation of O_2 in $Ic_{200}Pt_{9.98}H_1$ is that an activated oxygen species formed at the oxidation site could react with the carbon clusters to decrease the oxidation ability at the oxidation site, although no evidence was obtained yet to support this assumption.

Table 6
Amounts of O_2 and H_2 in water decomposition reaction under the irradiation of light ($\lambda > 460$ nm).

Materials	O_2 (mmol)	H_2 (mmol)	Ratio $[O_2]$:$[H_2]$
$Ic_{200}Pt_{9.98}H_1Mn_{57.5}$	127	255	1:2
$Ic_{200}Pt_{9.98}H_1$	0	145	–

4. Conclusion

We have succeeded in constructing an electron transfer enough to decompose water under visible light irradiation by

the calcination of a $Zr(acac)_4$/epoxy resin complex and successive surface modification with the Pt particles followed by the loading of the MnO_2 particles. The Pt-loaded material modified with MnO_2 particles could decompose water to H_2 and O_2 with a $[H_2]/[O_2]$ ratio of 2 under the irradiation of visible light ($\lambda > 460$ nm) through the electron transfer process of $MnO_2 \rightarrow$ carbon clusters $\rightarrow ZrO_2 \rightarrow$ Pt. We believe that similar photo-sensitive excitation could be achieved by the combination of carbon clusters and many other metal oxides, and our observations will contribute to develop many useful materials for the application in optical devices, oxidation–reduction catalysts, artificial photosynthesis catalysts, solar cell, and so on.

References

[1] K. Domen, J.N. Kondo, M. Hara, T. Takata, Photo- and mechano-catalytic overall water splitting reactions to form hydrogen and oxygen on heterogeneous catalysts, Bull. Chem. Soc. Jpn. 73 (2000) 1307–1331.

[2] R. Konta, T. Ishii, H. Kato, Photocatalytic activities of noble metal ion doped $SrTiO_3$ under visible light irradiation, J. Phys. Chem. B 108 (2004) 8992–8995.

[3] T. Ohno, D. Haga, K. Fujihara, K. Kaizaki, M. Matsumura, Unique effects of iron(III) ions on photocatalytic and photoelectrochemical properties of titanium dioxide, J. Phys. Chem. B 101 (1997) 6415–6419.

[4] N. Okada, S. Karuppuchamy, M. Kurihara, An efficient dye-sensitized photoelectrochemical solar cell made from $CaCO_3$-coated TiO_2 nanoporous film, Chem. Lett. (2005) 16–17.

[5] A. Kudo, H. Kato, I. Tsuji, Strategies for the development of visible-light-driven photocatalysts for water splitting, Chem. Lett. 33 (2004) 1534–1535.

[6] V. Etacheri, M. Seery, S. Hinder, S. Pillai, Highly visible light active $TiO_{2-x}N_x$ heterojunction photocatalysts, Chem. Matter 22 (2010) 3843–3853.

[7] H. Matsui, S. Yamamoto, T. Sasai, S. Karuppuchamy, M. Yoshihara, Electronic behavior of WO_2/carbon clusters composite materials, Electrochemistry 75 (2007) 345–348.

[8] S. Yamamoto, H. Matsui, S. Ishiyama, S. Karuppuchamy, M. Yoshihara, Electronic behavior of calcined material from a tantalum-O-phenylene-S-tin-S-phenylene-O hybrid copolymer, Mater. Sci. Eng. B 135 (2006) 120–124.

[9] T. Kawahara, H. Miyazaki, S. Karuppuchamy, M. Ito, M. Yoshihara, Electronic nature of vanadium nitride–carbon cluster composite materials obtained by the calcination of oxovanadylphthalocyanine, Vacuum 81 (2007) 680–685.

[10] T. Furukawa, H. Matsui, H. Hasegawa, S. Karuppuchamy, M. Yoshihara, The electronic behaviors of calcined materials from a (S-nickel-S-phenylene-O)-strontium-(O-phenylene-S-selenium-S) hybrid copolymer, Solid State Commun. 142 (2007) 99–103.

[11] T. Kawahara, T. Kuroda, H. Matsui, M. Mishima, S. Karuppuchamy, Y. Seguchi, M. Yoshihara, Electronic properties of calcined materials from a scandium-O-phenylene-O-yttrium-O-phenylene hybrid copolymer, J. Mater. Sci. 42 (2007) 3708–3713.

[12] H. Matsui, S. Karuppuchamy, J. Yamaguchi, M. Yoshihara, Electronic behavior of calcined materials from SnO_2 hydrosol/starch composite materials, J. Photochem. Photobiol. A: Chem. 189 (2007) 280–285.

[13] H. Miyazaki, H. Matsui, T. Nagano, S. Karuppuchamy, S. Ito, M. Yoshihara, Synthesis and electronic behaviors of TiO_2/carbon clusters/Cr_2O_3 composite materials, Appl. Surf. Sci. 254 (2008) 7365–7369.

[14] H. Matsui, K. Kira, S. Karuppuchamy, M. Yoshihara, The electronic behaviors of visible light sensitive Nb_2O_5/Cr_2O_3/carbon clusters composite materials, Curr. Appl. Phys. 9 (2009) 592–597.

[15] H. Matsui, K. Otsuki, H. Yamada, T. Kawahara, M. Yoshihara, Electron transfer behavior and water photodecomposition ability of calcined material from a cerium-S-phenylene-O-holmium-O-phenylene-S hybrid copolymer, J. Colloid Interface Sci. 297 (2006) 672–677.

[16] H. Matsui, T. Okajima, S. Karuppuchamy, M. Yoshihara, The electronic behavior of V_2O_3/TiO_2/carbon clusters composite materials obtained by the calcination of a $V(acac)_3$/$TiO(acac)_2$/polyacrylic acid complex, J. Alloy Compd. 468 (2009) L27–L32.

[17] H. Miyazaki, H. Matsui, Y. Kita, S. Karuppuchamy, S. Ito, M. Yoshihara, Electronic behavior of visible light sensitive ZrO_2/Cr_2O_3/carbon clusters composite materials, Curr. Appl. Phys. 9 (2009) 155–160.

[18] S. Ge, H. Jia, H. Zhao, Z. Zheng, L. Zhang, First observation of visible light photocatalytic activity of carbon modified Nb_2O_5 nanostructures, J. Mater. Chem. 20 (2010) 3052–3058.

[19] Y. Zhang, Z. Tang, X. Fu, Y.J. Xu, TiO_2-graphene nanocomposites for gas-phase photocatalytic degradation of volatile aromatic pollutant: is TiO_2-graphene truly different from other TiO_2-carbon composite materials, ACS Nano 12 (2010) 7303–7314.

[20] L. Wang, Y. Liu, M. Chen, Y. Cao, H. He, K. Fan, MnO_2 nanorod supported gold nanoparticles with enhanced activity for solvent-free aerobic alcohol oxidation, J. Phys. Chem. C 112 (2008) 6981–6987.